Surface & Coatings Technology 231 (2013) 277–280

Contents lists available at ScienceDirect

Surface & Coatings Technology

journal homepage: www.elsevier.com/locate/surfcoat

Transparent p-type Zn-doped $CuCrO_2$ films by sol–gel processing

Hong-Ying Chen *, Chun-Chao Yang

Department of Chemical and Materials Engineering, National Kaohsiung University of Applied Sciences, 415 Chiken Kuang Road, Kaohsiung 807, Taiwan, ROC

ARTICLE INFO

Available online 9 June 2012

Keywords:
Transparent conductive oxides
Delafossite
$CuCrO_2$
Sol–gel processing
Zn
Doping

ABSTRACT

This study reports the preparation of transparent p-type $CuCr_{1-x}Zn_xO_2$ ($x = 0.00, 0.01, 0.03$) wide-bandgap oxide semiconductor films deposited onto quartz substrates by a sol–gel process followed by a two-step annealing process. The films were first deposited onto quartz substrates by spin coating. The specimens were then annealed in air at 500 °C and post-annealed in N_2 at 700 °C for 2 h. The pure $CuCrO_2$ phase was obtained in $CuCr_{1-x}Zn_xO_2$ films with $x \leq 0.03$. The surface of the $CuCr_{1-x}Zn_xO_2$ films exhibited dense and elongated grains. The direct optical bandgaps of the $CuCr_{1-x}Zn_xO_2$ films were 3.0 eV ($x = 0.00$) and 3.05 eV ($x = 0.01$ and 0.03). The $CuCr_{1-x}Zn_xO_2$ films exhibited p-type characteristics with positive Seebeck coefficients. The electrical conductivities of $CuCr_{1-x}Zn_xO_2$ films were 0.15 S cm^{-1} ($x = 0.00$), 0.26 S cm^{-1} ($x = 0.01$), and 0.47 S cm^{-1} ($x = 0.03$). The corresponding hole concentrations of $CuCr_{1-x}Zn_xO_2$ films were 1.0×10^{18} cm^{-3} ($x = 0.00$), 2.0×10^{18} cm^{-3} ($x = 0.01$) and 3.2×10^{18} cm^{-3} ($x = 0.03$). The Zn doping of $CuCrO_2$ films can markedly enhance the electrical conductivity and hole concentration of the films. The Zn-doped $CuCrO_2$ thin films have the potential applications in transparent devices.

1. Introduction

Delafossite is a p-type wide-bandgap oxide semiconductor with the basic formula $A^IM^{III}O_2$, where A is Cu or Ag with monovalent cations and M is a trivalent metal ranging from Al to La [1]. The layered crystal structure has small-bandgap Cu_2O layers and large-bandgap $M^{III}{}_2O_3$ layers. These $M^{III}{}_2O_3$ layers enlarge the energy bandgap, resulting in a relatively large optical bandgap. Among these delafossite structure materials, $CuCrO_2$ has a relatively high electrical conductivity [1].

Wide-bandgap oxide semiconductors have become attractive in recent years because they are frequently used in optoelectronic applications. Transparent conducting oxides (TCOs), which are wide-bandgap oxide semiconductors, exhibit electrical conductivity and optical transparency in the same material [1,2]. This combination has numerous potential applications, including solar cells, flat panel displays, electromagnetic shielding devices, light-emitting diodes, and transparent heat sources. Currently, most popular wide bandgap TCOs, such as ZnO, In_2O_3, and SnO_2, exhibit n-type characteristics. However, p-type wide-bandgap TCOs are not well established, and have been relatively overlooked until recent years [1–5]. Various thin film deposition techniques have been employed for the deposition of delafossite materials [2–21]. $CuCrO_2$ films can be deposited using thin-film deposition techniques such as pulsed laser deposition [4–11], sputtering [12], chemical vapor deposition [13], and the sol–gel method [15–21].

Potential applications for p-type oxide semiconductors require crystalline films with high conductivity and hole mobility. Therefore, the incorporation of lattice defects, such as interstitial oxygen caused by oxygen intercalation, can increase p-conductivity [1,2]. However, oxygen intercalation has no effect on the electrical conductivity of $CuCrO_2$ films. This is because the interstitial oxygen defect is not stabilized in the limited interstitial site because of a small a-lattice parameter of the $CuCrO_2$ phase [1]. Doping is an alternative approach to increase the electrical conductivity and carrier concentration of these films. Substituting trivalent cations by divalent or trivalent cations in the structure significantly improve the electrical conductivity and carrier concentration of the films [5,8–12,14,15,17,18,20,21]. One of the selection rules for such dopants is similar ionic radii between dopants and host atoms, which minimizes the lattice distortion of the structure. In the $CuCrO_2$ phase, the ionic radius of Cr^{3+} is 0.0615 nm [22]. Therefore, it is necessary to select similar ionic radii of divalent cations. The ionic radii of Mg^{2+} and Zn^{2+} are 0.072 nm and 0.074 nm [22], respectively. The corresponding mismatches of ionic radii caused by the substitution of Cr^{3+} with Mg^{2+} and Zn^{2+} are 17.1% and 20.3%, respectively. Therefore, Mg^{2+} and Zn^{2+} are potential divalent dopants for the $CuCrO_2$ structure.

The Mg doping in $CuCrO_2$ thin films created a significant increase in the electrical conductivity of the films [5,8–11,14,15,20,21], resulting in the highest electrical conductivity in p-type delafossites [8]. Many Mg-doped $CuCrO_2$ films have been prepared by vacuum-based processing [5,8–11] and sol–gel processing [14,15,20,21]. In contrast, $CuCrO_2$ films doped with other divalent cations by sol–gel processing have not been well investigated. Additionally, the vacuum-based processes described previously are complex and time consuming. Substrate

* Corresponding author. Tel.: +886 7 3814526x5130; fax: +886 7 3830674.
E-mail address: hychen@cc.kuas.edu.tw (H.-Y. Chen).

0257-8972/$ – see front matter © 2012 Elsevier B.V. All rights reserved.
doi:10.1016/j.surfcoat.2012.06.006

heating and post-annealing are also required to improve the crystallization of the resulting films [9,11]. In contrast, the sol–gel method of preparing the wide-bandgap TCOs films has many advantages, including low cost, easy set up, large area coating, and mass production. Previous research has demonstrated that the sol–gel method is a powerful technique for growing delafossite films [16–21].

This study reports the fabrication of Zn-doped $CuCrO_2$ films prepared by the sol–gel processing. The sol–gel-derived films were annealed in air and post-annealed in N_2 to obtain a single $CuCrO_2$ phase. The microstructure of the $CuCr_{1-x}Zn_xO_2$ films was characterized by grazing incidence X-ray diffraction (GIXD) and field-emission scanning electron microscopy (FE-SEM). The optical properties were measured using an ultraviolet–visible (UV–vis) spectrometer, and the electrical properties of the films were investigated using Hall-effect measurements.

2. Experimental details

$CuCr_{1-x}Zn_xO_2$ ($x \le 0.03$) films with a delafossite structure on quartz substrates were prepared by the sol–gel process followed by two-step annealing. Specifically, copper(II) acetate (purity 98%+, Showa, Japan), chromium(III) acetate (EP grade, Showa, Japan) and zinc acetate (purity 98%+, Showa, Japan) were first dissolved in ethanol, and triethanolamine (purity 95%+, Tedia, USA) was then added to the solution. This precursor was then spin coated onto quartz substrates at 1000 rpm for 15 s. The specimens were then annealed at 500 °C in air for 1 h at a ramp rate of 5 °C/min before the next cycle. Three cycles were performed in this study. To obtain the single $CuCrO_2$ phase, the specimens were post-annealed at 700 °C in flowing N_2 (purity 99.9%, $pO_2 \sim 10^{-3}$ atm) for 2 h at a ramp rate of 5 °C/min.

A Bruker D8 Discover SSS X-ray diffractometer operating at 40 kV and 40 mA with Cu-Kα radiation ($\lambda = 0.154$ nm) was used to determine the crystal structure of the films. The operating mode was grazing incidence with an incidence angle of 1° and the sampled step size was 0.01° within $2\theta = 10$–70°. The surface morphology of the films was analyzed using an FE-SEM (JEOL JSM-6700F), and their optical properties were measured using a UV–vis spectrometer (Perkin Elmer Lambda 35). The electrical resistivity, carrier type, and carrier concentration of $CuCr_{1-x}Zn_xO_2$ films were assessed using standard Hall-effect measurements in the van der Pauw configuration at room temperature. Seebeck coefficient measurements were used to confirm the carrier type of the conduction in the $CuCr_{1-x}Zn_xO_2$ films.

3. Results and discussion

3.1. GIXD analysis

Fig. 1 shows the GIXD pattern of $CuCr_{1-x}Zn_xO_2$ films with $x = 0$, 0.01, and 0.03. This figure shows that the single $CuCrO_2$ (R3m, JCPDS #89-6744) phase is well defined. Strong (006), (012), and (110) diffraction peaks appear in the figure and their relative intensities remained constant as $CuCrO_2$ films were doped with different Zn contents. The values of the full width at half (FWHM) for the (006) diffraction peak were 0.25° ($x = 0.00$), 0.26° ($x = 0.01$), and 0.26° ($x = 0.03$). These narrow FWHM values represent good crystallinity in the $CuCr_{1-x}Zn_xO_2$ films.

3.2. FE-SEM analysis

Fig. 2(A) shows the surface morphology of $CuCr_{1-x}Zn_xO_2$ films with $x = 0.00$, 0.01, and 0.03. As illustrated in this figure, the surface of the $CuCr_{1-x}Zn_xO_2$ films consists of elongated grains features and dense structures. Similar features appeared in the Mg-doped $CuCrO_2$ films [21]. In the cross-sectional micrographs of $CuCr_{1-x}Zn_xO_2$ films in Fig. 2(B), the films are tightly attached to the substrate. Additionally, the films exhibit a morphology of granular stacks, with an average particle size of approximately 100 nm for all $CuCr_{1-x}Zn_xO_2$ films. The $CuCr_{1-x}Zn_xO_2$ films were approximately 190 nm ($x = 0.00$), 220 nm ($x = 0.01$), and 205 nm ($x = 0.03$) in thickness.

3.3. Optical properties analysis

The optical transmittance spectra of $CuCr_{1-x}Zn_xO_2$ films with $x = 0.00$, 0.01, and 0.03 were investigated at a wavelength of 350–900 nm (Fig. 3). The transmittance of the films in the visible region increases as the Zn concentration in the films increases, and the absorption edge of the films shifts to lower wavelengths. The average optical transmittances of $CuCr_{1-x}Zn_xO_2$ films in the visible region are approximately 47% ($x = 0.00$), 50% ($x = 0.01$), and 55% ($x = 0.03$). The low transmittance of the films may be the result of increased photon scattering by pores or grain boundaries in the films. The transparency in the visual region is also comparable to the films deposited by vacuum processing [6,9,10] and sol–gel processing [17,19,20] for un-doped or Mg-doped $CuCrO_2$ films.

Fig. 4 shows the optical bandgaps of $CuCr_{1-x}Zn_xO_2$ films with $x = 0.00$, 0.01, and 0.03. The fundamental of absorption, which corresponds to electron excitation from the valance band to the conduction band, can be used to determine the value of the optical bandgap of the films. The relationship between the absorption coefficients and the incident photon energy (hv) can be written as:

$$(\alpha h\nu)^n = A\left(h\nu - E_g\right) \quad (1)$$

where A is a constant, E_g is the bandgap of the films, hv is the photon energy, and α is the absorption coefficient. The value of n is 2 for the direct optical bandgap, and can be deduced from the portion of the plot to the hv-axis. The direct optical bandgaps of $CuCr_{1-x}Zn_xO_2$ films are 3.0 eV ($x = 0.00$), 3.05 eV ($x = 0.01$), and 3.05 eV ($x = 0.03$), respectively. The obtained direct optical bandgaps of the films are in good agreement with those reported in the literature [6,9,10,19,20].

3.4. Electrical properties analysis

Table 1 shows the electrical properties of $CuCr_{1-x}Zn_xO_2$ films. All of the $CuCr_{1-x}Zn_xO_2$ films in this study had positive Seebeck coefficients, confirming their p-type conductivity. The electrical conductivities of $CuCr_{1-x}Zn_xO_2$ films were 0.15 $S\,cm^{-1}$ ($x = 0.00$), 0.26 $S\,cm^{-1}$ ($x = 0.01$), and 0.47 $S\,cm^{-1}$ ($x = 0.03$) at room temperature.

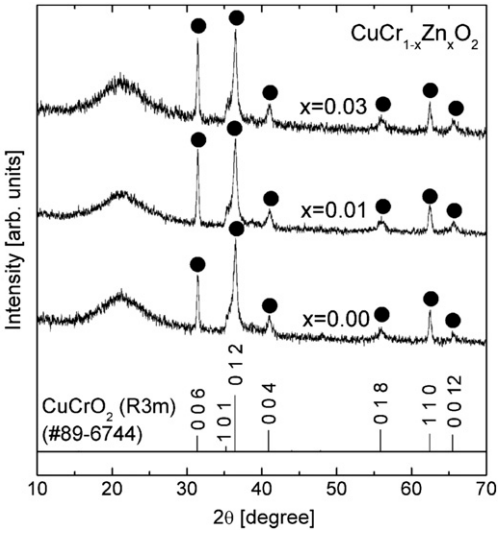

Fig. 1. GIXD patterns of $CuCr_{1-x}Zn_xO_2$ films with $x = 0.00$, 0.01, and 0.03.